ADJUSTMENT OF THE PARALLELISM OF TWO MIRRORS FOR WIDE ANGLE DIVIDED MIRROR MICHELSON WIND IMAGING INTERFEROMETER

Shaojun Lu[1, 2] and Chunmin Zhang[1]

1. School of Science, Xi'an Jiaotong University, Xi'an 710049, China.

2. School of Optical-electronic Engineering, Xi'an Technological University, Xi'an 710032, China

Email: huansc@126.com; hgyao1996@163.com

Submitted: Oct. 4, 2014 ***Accepted: Jan. 24, 2015*** ***Published: Mar. 1, 2015***

Abstract- ***Many ways have been developed to measure atmospheric winds by detecting the Doppler shifts of airglow emission lines. The Michelson Interferometer is widely used because of its simple principle. To get the Doppler shifts to calculate the wind velocity, researchers developed four-phase-step and divided mirror technology respectively. But they face challenges in many fields. So a wide angle Michelson Interferometer combining with divided mirror and phase stepping technique is used in this paper. A new algorithm is proposed in this paper to adjust the parallelism of the two mirrors for the Michelson Interferometer. Thus a high precision parallelism of the two mirrors can be obtained to get the phase shift and calculate wind velocity. The interval of the two mirrors has maximum difference less than one tenth wavelength. The experiments were performed in visible channel to prove the feasibility of this proposed algorithm. It can also be used in other fields demanding two surfaces parallel with high precision.***

Index terms: parallelism; phase shift; divided mirror; phase stepping

I. INTRODUCTION

The motion of air from high to low pressure caused by the changes in atmosphere temperature is called the geostrophic wind. Measurement of the wind helps to understand the dynamics of the stratosphere, and in essentially, understand the global distribution of ozone and other chemical species in the upper and middle atmospheric space. Many instruments have been developed to measure the wind velocity and its distribution. Doppler imaging is a typical way to measure winds in the atmosphere using airglow emissions through a field widened Michelson. The Wind Imaging Interferometer (WINDII) sponsored by the Canadian Space Agency and the French Centre National d'Etudes Spatiales, in collaboration with NASA, was launched in 1991 on UARS, the Upper Atmosphere Research Satellite[1]. It employs the natural airglow and auroral visible emission lines as sources and derives line-of-sight wind velocities from the Doppler line shifts by stepping the interferometer optical path difference in quarter wave steps[2-5]. It can get the wind pattern in the thermosphere and upper mesosphere using a Michelson interferometer with an imaging detector by widening the field of view and thermally compensating. But WINDII asks the stepping equipment to be high precise to obtain the optical path difference in quarter wave and have to change its step interval for different emission line. High-resolution Doppler imager (HRDI) is the other instrument on UARS, it measure winds in the upper troposphere, stratosphere and mesosphere using a triple-etalon Fabry-Perot spectrometer that observes the shifts of absorption lines in scattered sunlight. Some similar instruments based on Michelson Interferometer are developed for the other spectral regions to probe the wind down to the mesosphere and stratosphere. Mesospheric Imaging Michelson Interferometer (MIMI) is designed to monitor emission lines in the very bright O2 infrared atmospheric band at 1.27 μm to measure wind in different height ranges[6]. Its innovation lies in taking the phase images simultaneously by implementing a segmented mirror (with four quadrants at relative phases of $0^{\circ}, 90^{\circ}, 180^{\circ}, 270^{\circ}$)within the moving arm. The other particular advantage is using split filters to observe different emissions simultaneously. For measurements with the strong and weak sets of lines, it allows the relative intensities of the two sets of lines to be determined. Because of the difference in absorption for the two sets, density and pressure can be deduced assuming hydrostatic balance. But the disadvantages for MIMI are: 1)the relative phases between each quadrant are designed for fixed wavelength 1.27 μm, the changing in wavelength leads to coat again.2)It can

hardly obtain the rigid 90 degrees of phase interval by coating.3)It's not easy to measure the relative phases because of the infrared light. The Stratospheric Wind Interferometer for Transport Studies (SWIIFT) measures winds in the stratosphere from a satellite. It also develops a field-widened Michelson interferometer very similar to the WINDII instrument but operates in the mid-IR, where it detects the Doppler shifts of atmospheric thermal emission lines of ozone[7]. The piezoelectric system is used to adjust alignment. The Michelson Interferometer for Airglow Dynamics Imaging (MIADI) is developed to measure the two-dimensional wind to realize the wave observations in the Earth's mesosphere lower thermosphere (MLT) region[8]. The piezoelectric system is used to control the orientation and stepping of back mirror. A series of interferometer images is recorded to calculate the wind velocity, and experiment is done in lab. But the back mirror is not a segmented mirror, so can't record phase images simultaneously. The Waves Michelson Interferometer (WAMI) combining with divided mirror and phase stepping technique is developed to provide simultaneous measurements of dynamical and constituent signatures in the upper stratosphere, mesosphere and lower thermosphere by detecting visible and near-IR emissions simultaneously[9]. It obtains the four-step phase shifting by rigid 90 degrees more easily than MIMI and WINDII, since the deviation of 90 degrees in phase interval between each quadrant is permitted in this instrument. It can obtain the phase shifting of 90 degrees with a new algorithm combing with divided mirror and moving mirror. So it is significant for WAMI in fabricating because of its lower demanding in control of phase stepping and accuracy of coating for phase shifting.

To avoid the phase error caused by mirrors' interval, the two mirrors are demanded to be parallel with each other. Parallelism of two surfaces is necessary for many applications. For Michelson interferomenter, two mirrors should be parallel to get the fringes of white light. In modern microfabrication such as nanolithography, the parallelism of two surfaces are demanded to be the scale of microradians. Interferometry is very popular in adjusting the parallelism of two mirrors because of its uncontact and high precision[10,11]. A simple way to realize the parallelism of two mirrors is measuring their parallelism by laser interference technique for planes. Only one interferogram is recorded to get the numbers of fringes to get the parallelism. But it becomes invalid when the number of fringes is less than one. One fringe means the parallelism of two mirrors is a half wavelength. To realize parallelism with high precision, the phase-shifting interferometry has to be adopted to avoid the uncertainty caused by number of fringes less than

one[12]. It can measure the changes in interval of two mirrors as small as $\lambda/100$. The phase-shifting interferometry is realized by causing different additional phase in different time or space, and record the corresponding interferogram respectively, then calculate the phase from several interferograms to measure the parallelism[13-15]. Many methods have been developed as phase-shifting[16-19], for examples, by piezoelectric crystal, polarization, photoelectric crystal, changing wavelength, grating diffraction, etc. The piezoelectric ceramics PZT is used as phase-shifting equipment more frequently because of its mature technology. It can come to an accuracy of 0.01micrometer in displacement. But two things prevent its use in measuring the parallelism. One, a mechanical structure with high precision and sensitivity should be designed to get correct displacement without tilting. The other, the elongation caused by its deformation is not a rigid linear relationship with loaded electric field. So some compensation algorithms should be developed to reduce or eliminate its displacement error. Many algorithms have been proposed, including three-step and four-step phase shifting. But most of these algorithms require the two mirrors to be parallel.

In this paper, an algorithm is developed to calculate the phase difference between two mirrors in different area. An experiment equipment is designed to step the moving mirror with fixed orientation. Four sets of series of interferograms are recorded by CCD to calculate the phase difference. By adjusting the orientation of moving mirror, the maximum change in interval corresponding to phase difference of each area in the whole mirror is less than $\lambda/10$. It proved the two mirrors have more higher accuracy in parallelism compare with one interferogram.

II. WIND MEASUREMENT WITH VISIBLE CHANNEL OF WAMI

A. Visible channel of WAMI

It is easy to be controlled by human being, so the experiment is done in visible channel with laser at 632.8nm. The optical configuration of WAMI in visible channel is shown in figure1.The parallel light coming from infinity oxygen emission lines illuminates the field stop and is divided by beam splitter into two beams. The exiting two beams interference and form Haidinger fringes at infinity, so a lens with a CCD located on the focal plane is used to record the fringe pattern. By sampling the fringes we can get the phase shift between the zero wind and detected wind velocity.

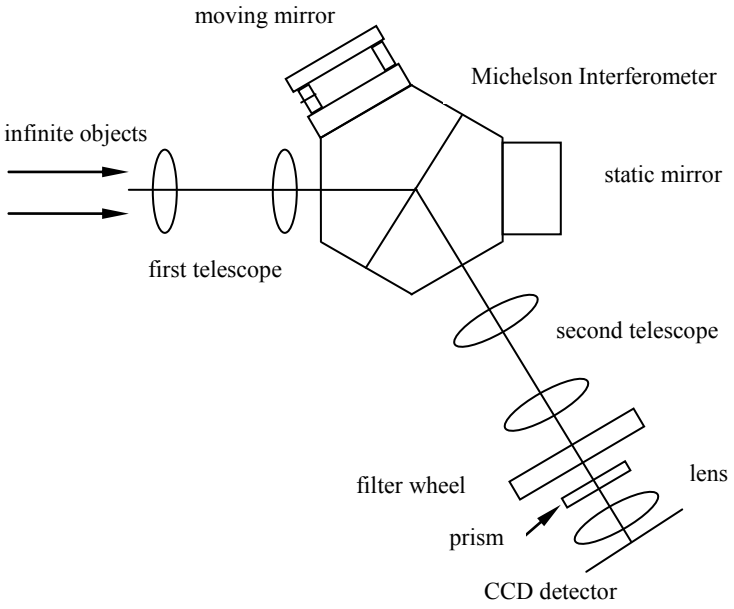

Figure 1 The visible channel of WAMI

The Michelson Interferometer is critical for this equipment, has a segmented moving mirror at the bottom of one arm and a fixed mirror in the other arm. Two arms are glasses, SF11 and LaKN12 respectively, cemented on two half-hexagons of BK7 glass. Thus it can achieve field widening and thermal compensation at two widely separated wavelengths. The moving mirror mounted on piezoelectrics to control its position and alignment through a feedback loop. It uses capacitors to sense the gap between moving mirror and SF11 glass. Considering the visibility in the interferogram and the effective emission temperature, the path difference was chosen to be 6 cm.

The entrance aperture is just ahead of the first telescope. The first telescope defines the field of view as $4.5^\circ \times 4.5^\circ$, and projects the light through the Michelson, focusing the entrance aperture at the interferometer's mirrors. The second telescope focuses the mirrors at two shallow, pyramid shaped prism behind the filters, in front of CCD detector. The edges of the prism are aligned with the divisions between the quadrants of the sectored Michelson mirror, so the light from each sector is diverted in a different direction, forming four images on CCD detector, one for each sector of the Michelson mirror. The entrance aperture is 5 cm in diameter and the effective aperture ratio for the optical system is f/1.3. The magnification of the first telescope is 2 and of the second 0.5, so the field of view at the Michelson is $9^\circ \times 9^\circ$ and at the filters is again $4.5^\circ \times 4.5^\circ$ [9].

The emission line from infinity through the telescope entering the interferometer is divided into two components along two arms. Then two beams reflected by two mirrors come together through the beam splitter and form interference pattern on CCD detector.

B. The principle for measuring wind

The oxygen green line emission ($O(^1S)$) at 557.7 nm and lines in the (0-0) vibrational transition of the O2 infrared atmospheric band ($O_2(^1\Delta)$) near 1270 nm are chosen to be moving sources probed by WAMI. The Doppler shifts in the spectral line center of isolated emission lines from a moving source can be achieved from phase changing by exploiting fringes of an interferogram. The Haidinger fringes are imaged on CCD detector device and sampled while the interferometer is scanned. The interference intensity recorded on CCD can be described by equation(1).

$$I(\Delta) = I_0[1 + UV\cos(2\pi\sigma_0\Delta)] \tag{1}$$

Where I_0 is the mean value of the measured intensity, U the instrument visibility, V the line visibility depended on the line shape and width of the source, σ_0 the wave number of central emission line referring to the zero wind velocity, Δ the path difference introduced between the beams exiting the interferometer. If the source has a line-of-sight velocity υ relative to the observer, the Doppler shift occurs. The wave number σ can be written as

$$\sigma = \sigma_0(1 + \upsilon/c) \tag{2}$$

Where c is the velocity of light. The phase of fringes $\phi = 2\pi\sigma\Delta$ depends on the wavelength or wind velocity. This Doppler shift makes the path difference Δ has a small change due to dispersion in the interferometer glass, it can be written as $\Delta = \Delta_0 + \Delta'$ .Where Δ_0 can be chosen to get $\cos(2\pi\sigma_0\Delta_0) = 1$, Δ' the changing in path difference. Substitute them in equation(1), we can get

$$I(\Delta') = I_0[1 + UV\cos(2\pi\sigma_0\Delta' + \phi)] \tag{3}$$

and

$$\phi = 2\pi\sigma_0 D\upsilon/c \tag{4}$$

Where D is the effective path difference[20]. Wind velocity can be determined from the phase ϕ, and ϕ can be calculated in the following way. If we increase Δ' in steps of quarter wavelength from $\Delta' = 0$, the corresponding four detected intensities I_1, I_2, I_3, I_4 can be used to solve ϕ from equation(5).

$$\phi = \tan^{-1} \frac{I_1 - I_3}{I_4 - I_2} \tag{5}$$

WINDII changes the path difference by the scanning mirror, but MIMI by divided mirror technique. But for all the equipments, there are some errors for each step interval. And the more the deviation in step distance from quarter wavelength, the more error in wind velocity occurs. For this equipment, the principle to measure wind velocity is the same as the four-intensity algorithm, but the combination of segmented mirror and the piezoelectric system make it is more accurate to obtain the 90 degrees' phase interval. So the piezoelectric system is used in WAMI to try to get the 90 degrees of phase shift to achieve high precision in wind velocity by calculating the phase of each step and each quadrant. The principle to get phase is introduced in the following section.

III.THE PRINCIPLE TO ADJUST THE PARALLELISM OF TWO MIRRORS

A. Equal thickness fringes

Equal thickness fringes occur near a thin layer when the two mirrors have a tiny angle and collimated light came from a point source is used in Michelson interferometer. It is also called as Fizeau fringes, a localized interference pattern. In a field widened Michelson interferometer, one mirror and the virtual image of the other mirror form a thin virtual flat when the distance of one mirror to beam splitter and the other mirror to beam splitter is close to each other. The light reflected by two mirrors come together to interference, its fringe pattern can present the surface information of two mirrors. If there are non-uniformities in the mirrors, the beams coming from different point in the mirror would have slightly different path difference and a measure of the phase difference across the image would give an estimate of the non-uniformity across the minors. So the equal thickness fringes can be used to adjust the parallelism.

The experimental setup to record the equal thickness fringes is shown in figure2. The laser produces monochromatic light. Diffuser and ground glass form uniformed intensity disc on small hole, which can be regarded as a point source. The beam exiting from collimator coming from the small hole is approximately collimated light. It is divided into two beams by the beam splitter. The two beams reflected by two mirrors are coherent light. When there are a tiny angle between the two mirrors of the virtual flat formed by a mirror and the virtual image of the other mirror, the parallel linear fringes will occur near the flat. The interval of the linear fringes represents the

amount of the angle. The CCD detector focuses on the position of segmented mirror to record the interference pattern occurred near the virtual flat.

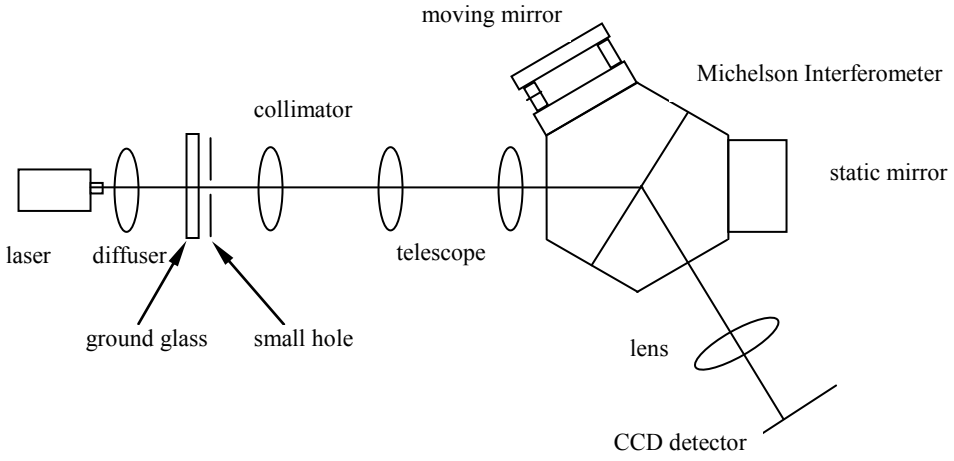

Figure2. The experiment to produce and record the equal thickness fringes

B. The principle to obtain phase

When two mirrors are parallel with each other, the whole space between them has the same distance. For the field-widen Michelson interferometer with segmented mirror, all points in each quadrant have the same phase difference. So we can adjust the parallelism by comparing the phase difference. But it will take too much time to calculate the phase for all points corresponding to the CCD pixels. In each quadrant a square consist of 5×5 pixels is regarded as a point, average value of each square is obtained.

If we scan the moving mirror j times with i steps, suppose the intensity A^j, visibility V^j and phase θ^j are fixed for the ith step and the phase φ_i is fixed for the jth scan, the mathematical interference intensity recorded on the CCD can be written as equation(6).

$$I_i^j = A^j(1+V^j\cos(\theta^j+\varphi_i)) \tag{6}$$

For the instruments using the four-step phase shifting algorithm such as WINDII and MIMI, the phase $\varphi_i = 0,\pi/2,\pi,3\pi/2$, $i=1,2,3,4$. In the jth scan, the intensity A^j, visibility V^j and phase θ^j can be calculated from the four intensities detected by CCD. So the phase θ^j corresponding to zero wind and detected wind velocity can be calculated respectively, the wind velocity can be obtained with equation(4). As mentioned above, these equipments have errors in phase shifts for each step. It will cause deviation in measured wind velocity. So a Least Mean Square algorithm is developed

by W.E.Ward[21] to calculate the values by j scans and i steps over a period in fringes. Only require that the two mirrors are parallel, don't need the step interval is rigid quarter wavelength. There are some changes for this algorithm in this paper, the intensity A^j, visibility V^j and phase θ^j are regarded as the values for each point (in fact, each square here), and the phase ϕ_i is the phase for each step. There are four quadrants in the moving mirror, one scan for this equipment can get four different values of A^j, V^j and θ^j, just like four scans as the WINDII. To get the phase of different squares, we can choose 100 points in the image to calculate the values of A^j, V^j and θ^j. At least steps are adopted in this experiment to make the interference fringe for the wavelength at 632.8nm is more than one period.

x_i^j is used to represent the recorded interference intensity of each point, S the sum of the square difference between the detected values and model values from equation(6). S can be written as

$$S = \sum_{j=1}^{100}\sum_{i=1}^{20}(x_i^j - I_i^j)^2 = \sum_{j=1}^{100}\sum_{i=1}^{20}(x_i^j - A^j(1 + V^j\cos(\theta^j + \varphi_i)))^2 \tag{7}$$

An iterative algorithm is adopted to calculate the values. Calculate the deviations in equation(8) and set to zero.

$$\frac{\partial S}{\partial \phi_k}, \frac{\partial S}{\partial \theta^l}, \frac{\partial S}{\partial V^l}, \frac{\partial S}{\partial A^l} \tag{8}$$

By supposing the initial values of 20 ϕ_i and substituting for them in the equations calculated from equation(7), then calculate the value of S, until the difference is less than a specified value. The values of A^j, V^j, θ^j and ϕ_i can be obtained. So in this way, the step size may be an arbitrary value and the number of steps is an arbitrary number making the fringe over than one period. If the step size is known just like WINDII, it is more easy to calculate the values of A^j, V^j, θ^j.

Ⅳ. EXPERIMENT AND DATA ANALYSIS

A. MALICE system

Just as mentioned above, because of the algorithm above is developed to calculate the values of A^j , V^j , θ^j and ϕ_i ,the step size is arbitrary for the moving mirror. But the two mirrors should be parallel during stepping the moving mirror. So a system should be designed to adjust the orientation of moving mirror and keep its orientation during stepping. Thus we can calculate the phase corresponding to disalignment of the two mirrors and find the difference to adjust the orientation of moving mirror to obtain the final parallelism. The multi-application low-voltage piezoelectric instrument control electronics (MALICE) and its control software developed by COM DEV Ltd is used to realize the requirement above.

MALICE is a multi-application package that includes a digital signal processor with programmable software parameters that must be matched with the physical characteristics of the optics being positioned[8]. For example, the MALICE system has been implemented to orient and position the scanning mirror of Fabry-Perot etalons[22,23]. A Windows graphical user interface (GUI) is used to Communicate with the interferometer. And a UARTS RS-232 data packet is used to send commands to the system. A calibrated stepping profile, sent to the MALICE system, is stored in the hardware and can be accessed by reading and applying 0–5 V TTL signals to the two 15 pin control in and out connections on the back of the unit. The MALICE system interfaces with and controls the configuration of the air gap arm in the WAMI interferometer. This is depicted schematically in Fig. 3 and the corresponding simplified electronic diagram is shown in Fig. 4. Five identical gold plated capacitors (labeled by C) and three low voltage piezoelectric actuating cylinders (labeled by PZT) are geometrically positioned in the air gap arm of the interferometer. Orthogonal pairs of identical capacitors C3, C5 and C1, C4 are wired into a capacitance bridge system as Channel 1 (CH1) and Channel 2 (CH2), facilitating the control of tilts of the interferometer scanning mirror about orthogonal axes in the XY plane (the plane orthogonal to the optical axis of the system). A low-drift ceramic capacitor (Cref) is paired with C2 to provide the "Z" air-gap channel that measures mirror displacement along the optical axis on Channel 0 (CH0). Each channel provides a high frequency digitized error signal (SX, SY, and SZ) output from the capacitance bridge system. The calibration process requires the user to manually position the

mirror in a series of parallel steps. For each position, the MALICE system software will then determine a high precision calibrated "set point" waveform (VX, VY, and VZ) with phase and amplitude that zero the corresponding output errors, corresponding to each particular mirror gap and orientation. These set points correspond to a balanced capacitance bridge system (error minimum). When a scanning profile of set points and hold times is given to MALICE, the three low-voltage piezoelectric actuating cylinders maintain the calibrated air gaps for the specified times and are actively controlled in software to minimize the error signals and thus locate the unique mirror position and orientation. The MALICE GUI can be used to retrieve the set point corresponding to a particular mirror position and orientation using the built in auto-calibration routine. The raw error signals can also be accessed through the interface. The procedures and techniques developed and applied to this equipment to obtain a one-to-one mapping of set point to adjust the parallelism of two mirrors.

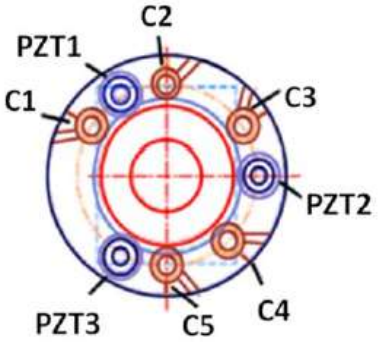

Figure 3. Placement of capacitors (C) and piezoelectric posts (PZT) in the mirror side of the air gap arm of the WAMI interferometer

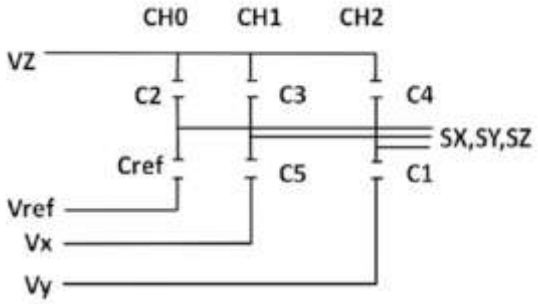

Figure 4. Three channel capacitance bridge system formed by the arrangement

B. Experiment to adjust the parallelism

Experiments have been done in laboratory to adjust the parallel of the two mirrors of Michelson interferometer with the MALICE system. The moving mirror is controlled to move without tilting. Don't need to know exactly the step size. The values of A^j , V^j , θ^j and ϕ_i can be obtained with the algorithm mentioned above.

1) Turn on the laser to get stable exit intensity. Turn on and cool the CCD to keep a lower temperature at -20 degrees to get lower noise.

2) Get a dark image as background by covering a lid at the field stop, so no incident light can pass through the instrument but surrounding light can be detected. The expected signals should be the detected intensity of fringes subtracted by the background.

3) Adjust the experiment system described by figure2 to achieve equal thickness fringes to approximately adjust the parallelism. To form the image of linear fringes on CCD, focus the lens near the virtual flat composed by two mirrors. In this equipment with segmented back mirror, CCD can be focused on the back mirror when the segmented line is clear. Reduce the size of small hole to get approximately collimated light and form the clear cross segmented line of on the image. The image is shown in figure5.

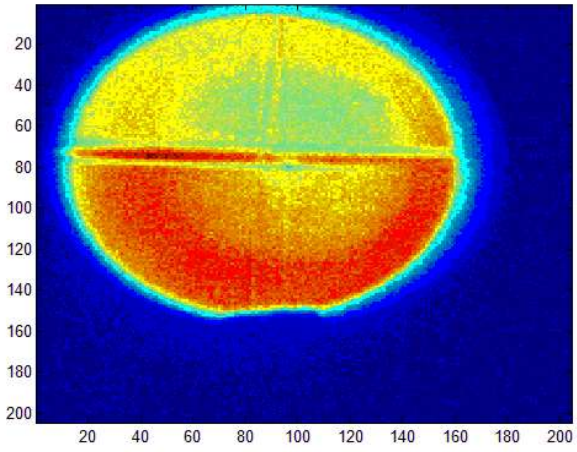

Figure 5. The clear cross line of back mirror

4) Choose the initial parameters of the MALICE system to observe the equal thickness fringes. The initial parameters of the channel 0, 1 and 2 are obtained by adjusting the orientation of moving

mirror and observe the equal thickness fringes for a long time. Then keep the orientation of the mirror and step it, the fringes will move in the field of view. Change the parameters of XY plane in MALICE system to adjust the orientation of the back mirror with tilting. The parallel linear fringes can be seen on CCD firstly and then the fringes disappear little by little till the linear fringes can't be observed. For the traditional way to adjust the parallel, the two mirrors may be regarded as parallel.

5) Keep the orientation of the back mirror, step the moving mirror with arbitrary size and numbers of steps only assuring the fringe is longer than one period. Considering the wavelength at 632.8nm and the size corresponding to each step controlled by this MALICE system, at least 20 steps are moved in this experiment. During the experiment, channel 0 is fixed, while channel 1 and channel 2 are free, so increasing the number in the parameters of channel 0 one each time, and the mirror will change the identical gap without tilting in XY plane. To obtain the correct values of A^j, V^j, θ^j and ϕ_i, the phase shift lies in different profiles of fringes in each quadrant. Four curves of the detected fringes in four quadrants are shown in figure6 with different colors. As has been proved, the more the phase shift is close to 90 degrees, the more precise for the detected values. The film on segmented mirror is coated for the wavelength at 1.27μm instead of 632.8nm to get phase shift of 90 degrees, so in figure6 the phase shift between two neighbor quadrants is almost 180 degrees.

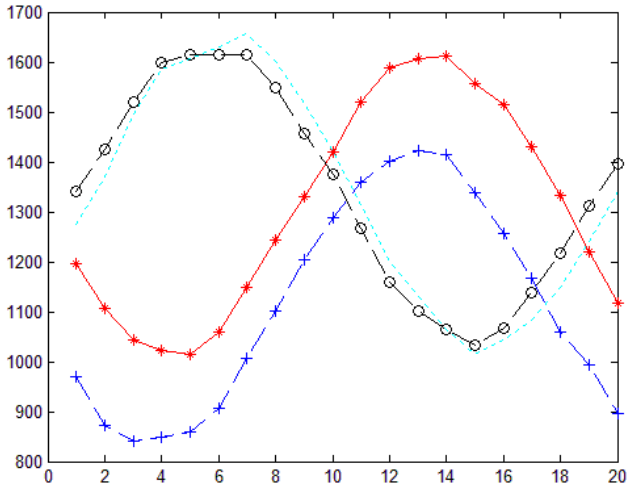

Figure 6. The intensity versus steps in four quadrants

In figure6, the red line is the intensities in the upper-left quadrant, the black the upper-right, the blue the lower-left and the green the lower-right.

6) Suppose the initial values of phase ϕ_i ($i = 1,2,3\cdots 20$), the algorithm mentioned above is used to solve the values of A^j, V^j, θ^j and ϕ_i. There are certain phase shifts between each neighbor quadrant, so for the phase ϕ_i of a certain step, the phase θ^j of each quadrant will have great changes. From which we can't judge whether the two mirrors are parallel or not. In each quadrant, 25 points in the bright area of figure5 are selected to calculate the phase θ^j and compare the values to judge the parallelism. One point in fact represents a square of 5×5 pixels. 100 values of θ can be obtained to observe the parallelism. And in each quadrant, the choice of the 25 points should cover the bright area as possible. The curve of the relationship between the calculated ϕ_i ($i = 1,2,3\cdots 20$) and their steps is plotted in figure6.

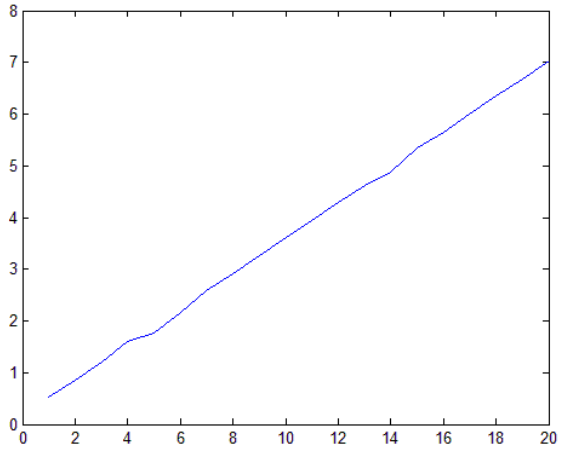

Figure 6. The relationship of phase and step

The calculated values of θ are shown in figure7, 100 squares in figure7 represent the 100 points selected. The different colors mean different values. The upper-left and the lower-left quadrant have an opposite phase because of the 180 degrees of phase shift. We can find the maximum phase shift in each quadrant is almost the same, which means the film coated is uniform for each quadrant. The inclination for the phase changes from minimum to maximum is almost the same, which means the mirror has the same tilt for the four quadrants. The calculated maximum values of the four quadrants are 0.6984, 0.5575, 0.5236, 0.4719 respectively. Considering the twice

relationship of the path difference and distance of two mirrors, Use the equation $\delta h = \frac{\delta\varphi}{4\times\pi}$, the phase difference can be changed to the unit of wavelength:0.0556,0.0444,0.0417,0.0376. So the maximum height difference in one quadrant is nearly $\lambda/20$. The values of phase for the initial parameters obtained from one interferogram are: 0.8628, 0.6058, 0.3468and 0.6163. The corresponding phase values of all points are shown in figure8. We can find the phase difference becomes smaller after adjusting.

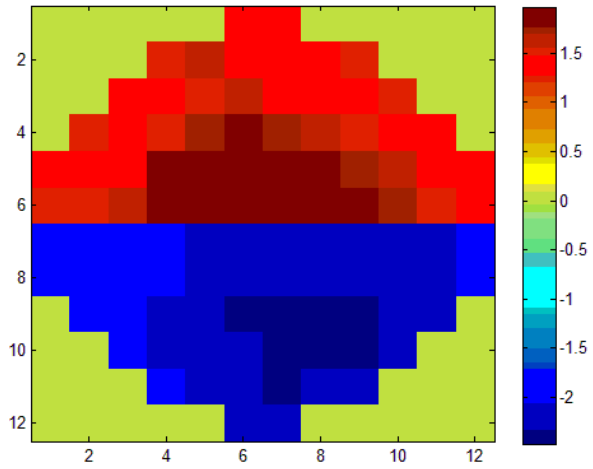

Figure 7. Calculated phases in four quadrants for parallelism

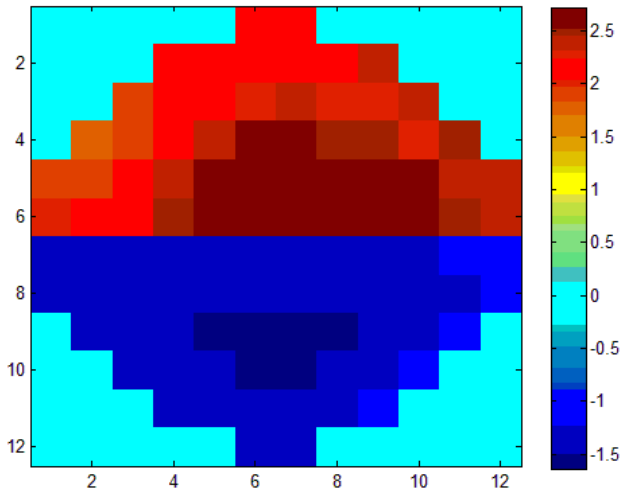

Figure 8.Calculated phases for initial parameters

V. CONCLUSIONS

The MALICE system is introduced in the visible channel of WAMI to control the orientation of the moving segmented mirror to step with arbitrary size. A reiterate algorithm is developed to calculate the parameters of the interference fringes, especially the phase of each point to adjust the parallelism of the two mirrors. By adjusting the orientation of the moving mirror and step it, the two mirrors can get high precision in parallelism comparing with one inter-ferrogram. The maximum difference in distance of the two mirrors reaches to $\lambda/20$, less than the phase shifting way of $\lambda/100$. But this instrument doesn't demand exactly for the stepping equipment in size. And combining with the segmented mirror and MALICE system, it may be more easy and accurate to obtain the 90 degrees of phase shift to measure wind velocity with four-step phase shifting way. It can also be used to test the uniform of the film coated for phase shift and detect the value of the phase interval between the neighbor quadrants.

After adjusting the parallelism of the two mirrors, we can design simulated wind to measure wind velocity. This technique can be used in the field of vehicle detection and 6-axis industrial for high accurate adjusting of the equipment.[24-28]

The experiment is carried on at the lab in University of New Brunswick in Canada, give thanks to professor W.E. Ward for his support and explanation for the algorithm and the principle of the instrument. Give thanks to his doctorial student Jeffery for his support in operating the instrument.

REFERENCES

[1]G. G. SHEPHERD, G. THUILLIER, W. A. GAULT, etc. "WINDII, the Wind Imaging Interferometer on the Upper Atmosphere Research Satellite", JOURNAL OF GEOPHYSICAL RESEARCH, Vol.98, No.D6, pp.10,725-10,750, June1993.

[2]Gordon G. Shepherd, William A. Gault, D. W. Miller, etc., "WAMDII: wide-angle Michelson Doppler imaging interferometer for Spacelab", Applied optics, Vol.24, No11.pp.1571-1584.1985.

[3]Shengpan P. Zhang, Gordon G. Shepherd, "Aurora and diurnal tides in the daytime O(^{1}S) emission rates from WINDII/UARS measurements", SPIE. Vol. 5979, pp.597911-1-7.

[4] S. P. Zhang and G. G. Shepherd, " On the response of the O(^{1}S) dayglow emission rate to the

Sun' s energy input: An empirical model deduced from WINDII/UARS global measurements," J. Geophys. Res.Vol.110, pp.A03304. 2005.

[5] C. Lathuill`ere,W. A. Gault, B. Lamballais, Y. J. Rochon, and B. H., "Solheim. Doppler temperatures from O(^{1}D) airglow in the daytime thermosphere as observed by the Wind Imaging Interferometer (WINDII) on the UARS satellite", Annales Geophysicae. Vol.20, pp.203-212. 2002.

[6] DAVID D. BABCOCK, "Mesospheric Imaging Michelson Interferometer Instrument Development and Observations", TORONTO: YORK UNIVERSITY.2006.

[7] William Gault, Ian McDade, Gordon Shepherd, etc., "SWIFT: an infrared Doppler Michelson interferometer for measuring stratospheric winds", SPIE.Vol.4131,pp.96-107,2001.

[8] Jeffery A. Langille, William E. Ward, Alan Scott, and Dennis L. Arsenault, "Measurement of two-dimensional Doppler wind fields using a field widened Michelson interferometer", Applied optics, Vol.52, No.8, pp.1617-1628, 2013.

[9] William E. Ward, William A. Gault, Gordon G. Shepherd, and Neil Rowlands, "The Waves Michelson Interferometer: A visible/near-IR interferometer for observing middle atmosphere dynamics and constituents", SPIE, Vol.4540, pp.100-111, 2001.

[10] J. H. Bruning, D. R. Herriott, et al., "Digital wavefront measuring interferometer for testing optical surfaces and lenses", Applied optics, Vol.13,No.11, pp.2693-2703,1974.

[11] K. Pramod. Rastogi, "Optical Measurement Techniques and Application", Boston: Artech House, 1997.

[12]G. Lai and T. Yatagai, "Generalized phase-shifting interferometry", J. Opt.Soc.Am.(A), Vol.8,No.5,pp.822-827,1991.

[13]Peter de Groot, "Measurement of transparent plates with wavelength-tuned Phase-shifting interferometry", Applied Optics, Vol.39, No.16, pp.2658-2663.2000.

[14] Y. Ishii, R. Onoder, "Phase-shifting interferometer for distance measurement using a Tunable external-cavity laser diode", SPIE, Vol.3749, pp. 436-437, 1999.

[15] P. Hariharan, B. F. Oreb, and T. Eyui. Digital phase-shifting interferometry: a simple error-compensating phase calculation algorithm. Appl. Opt. Vol.26, No.13, pp.2504-2506, 1987.

[16] J. Schmit and K. Creath, "Extended averaging technique for derivation of error-compensating algorithms in phase-shifting interferometry", Appl. Opt.Vol.34, No.19, pp.3610-3619, 1995.

[17]M. Servin, D. Malacara, J. L. Marroquin and F. J. Cuevas, "Complex linear filters for phase shifting with very low detuning sensitivity", J. Mod. Opt, Vol.44, pp.1269-1278, 1997.

[18] K. G. Larkin and B. F. Oreb, “Design and assessment of symmetrical phase-shifting algorithms”, J. Opt. Soc. Am. (A), Vol.9, pp.1740-1748, 1992.

[19] M. Miranda and B. V. Dorrio, “Fourier analysis of two-stage phase-shifting algorithms”, J.Opt. Soc. Am. A, Vol.27, No.2, pp.276-285, 2010.

[20] C. Anderson, M. Conde, and M. G. McHarg, “Neutral thermospheric dynamics observed with two scanning Doppler imagers: 1.Monostatic and bi-static winds,” J.Geophys.Res, Vol.117, A03304, 2012.

[21] W. E. Ward, “Design/Implementation of a WAMI to observe thermosphere winds,” PhD thesis, York University, Ontario.1988.

[22] A. Scott, R. Norman, and L. Zhou, “Tunable etalons and other applications of MALICE,” SPIE, Vol.5492, pp.1755, 2004.

[23] G. Sen Gupta, S.C. Mukhopadhyay and M Finnie, Wi-Fi Based Control of a Robotic Arm with Remote Vision, Proceedings of 2009 IEEE I2MTC Conference, Singapore, May 5-7, 2009, pp. 557-562.

[24] E. Mentuch, A. Scott, R. Abraham, E. Barton, M. Bershady, J. Bland-Hawthorn, D. Crampton, R. Doyon, S. Eikenberry, M. Gladders, K. Glazebrook, J. Jenson, J. Julian, R. Julian, J. Kneib, D. Loop, N. Raines, N. Rowlands, and J. D. Smith,“Optical-mechanical operation of the F2T2 filter: a tunable filter designed to search for first light,” SPIE,Vol.7014,pp.76, 2008.

[25] I. Emerson, W.L.Xu, S.C.Mukhopadhyay, J.C. Chang and O. Diegol, “Robotic Rehabilitation System for Stroke in Combination with Mirror Therapy: A Research Proposal”, Proceedings of the 25th International Conference of CAD/CAM, Robotics and Factories of the Future, ISBN 978-0-620-46582-3, July 13-16, 2010, Pretoria, South Africa, 12 pages.

[26]Yiling Chen, GuoFeng Qin, “Video-based vehicle detection and classification in challenging scenarios,” International Journal on sSmart Sensing and Intelligent System, Vol.7, No.3, September 2014.

[27] G.Sengupta, T.A.Win, C.Messom, S.Demidenko and S.C.Mukhopadhyay, “Defect analysis of grit-blasted or spray printed surface using vision sensing technique”, Proceedings of Image and Vision Computing NZ, Nov. 26-28, 2003, Palmerston North, pp. 18-23.

[28]Jianhao Zhang, Jinda Cai, “Error Analysis and Compensation Method of 6-axis Industrial Robot,” International Journal on Smart Sensing and Intelligent System, Vol.6, No.4, September 2013.